

Article

Double-Sided Self-Pierce Riveting: Electro-Mechanical Analysis of Dissimilar Al-Cu Half-Lap Butt Joints

Rafael M. Afonso * and Luís M. Alves * 

IDMEC, Instituto Superior Técnico, University of Lisbon, Av. Rovisco Pais, 1049-001 Lisbon, Portugal

* Correspondence: rafael.afonso@tecnico.ulisboa.pt (R.M.A.); luisalves@tecnico.ulisboa.pt (L.M.A.)

Abstract: Double-sided self-pierce riveting (DSSPR) can be utilized as an alternative to self-pierce riveting (SPR) to produce butt joints through half-lap joints in dissimilar materials. The mechanical joining process makes use of tubular rivets with simple geometry that are here employed to join two sheets made from aluminium (Al) and copper (Cu). This research work analyses the influence of the stainless-steel rivet on both the electrical and mechanical performance of the joint. The electrical resistance variation of the joined assembly is measured at different temperatures and compared with conventional fastened joints made from the same material combination. The mechanical performance of the aluminium–copper connections is evaluated by means of shear tests and compared to the original fastened Al-Cu joint. An experimental approach is utilized to analyse the combined influence of different mechanical and electrical parameters to assess the performance of DSSPR in electrical applications.

Keywords: joining technology; mechanical joints; butt joints; sheets; self-pierce riveting; electro-mechanical performance

1. Introduction

Difficult design challenges arise from the need of industry to produce joints between aluminium and copper with laser welding to create a connection between different battery cells. The reason for the interest in joining these two materials is related to many aspects such as the higher strength of the joints produced along with lower levels of electrical resistance and heat generated [1]. Busbar systems made from dissimilar materials need then to be obtained with a simplified and lower cost approach that is able to offer high reliability, repeatability and performance.

For the production of these busbar systems, butt joints are normally produced by means of soldered joints, which can lead to defective joints that result from different metallurgic alterations produced during the fabrication process [2]. To bypass the utilization of welding processes, joining by forming processes [3] can be utilized to produce different mechanical joints [4,5]. From these techniques and to fulfil the requirements of lower contact resistance, the contact surface needs to be increased. Therefore, the production of butt joints through means of a double-sided self-pierce half-lap riveted joint is proposed in this paper. This strategy allows us to combine the advantages of both lap and butt joints, since it extends the contact surface between the materials, which is limited to the side walls of the sheets for butt joints, while it allows the creation of a seamless upper and lower surface without protrusions, as is normally verified for lap joints, which, in turn, are able to offer a larger contact region and additional contact points between the sheets.

Double-sided self-pierce riveting (DSSPR) has been investigated by the authors in recent years, and different joining strategies have been developed [6] to handle different combinations of materials [7] and thicknesses [8]. As the name implies, a double-sided tubular rivet is employed to produce a mechanical joint between sheets (Figure 1a). In comparison with self-pierce riveting (SPR) [9], which is depicted in Figure 1b, DSSPR



Citation: Afonso, R.M.; Alves, L.M. Double-Sided Self-Pierce Riveting: Electro-Mechanical Analysis of Dissimilar Al-Cu Half-Lap Butt Joints. *Metals* **2023**, *13*, 1472. <https://doi.org/10.3390/met13081472>

Academic Editor: Guido Di Bella

Received: 23 July 2023

Revised: 8 August 2023

Accepted: 11 August 2023

Published: 15 August 2023



Copyright: © 2023 by the authors. Licensee MDPI, Basel, Switzerland. This article is an open access article distributed under the terms and conditions of the Creative Commons Attribution (CC BY) license (<https://creativecommons.org/licenses/by/4.0/>).

produces a joint with a non-exposed rivet of simple geometry that remains hidden between the sheets without tearing up any of these materials during the joining process. For this joining by the forming process, a tubular rivet with chamfered ends is forced to penetrate the sheets as they are compressed against each other. This deformation increases the strain hardening levels of the materials from the sheets, which forces the rivet ends to flare, thus creating a mechanical interlocking (refer to Figure 1a).

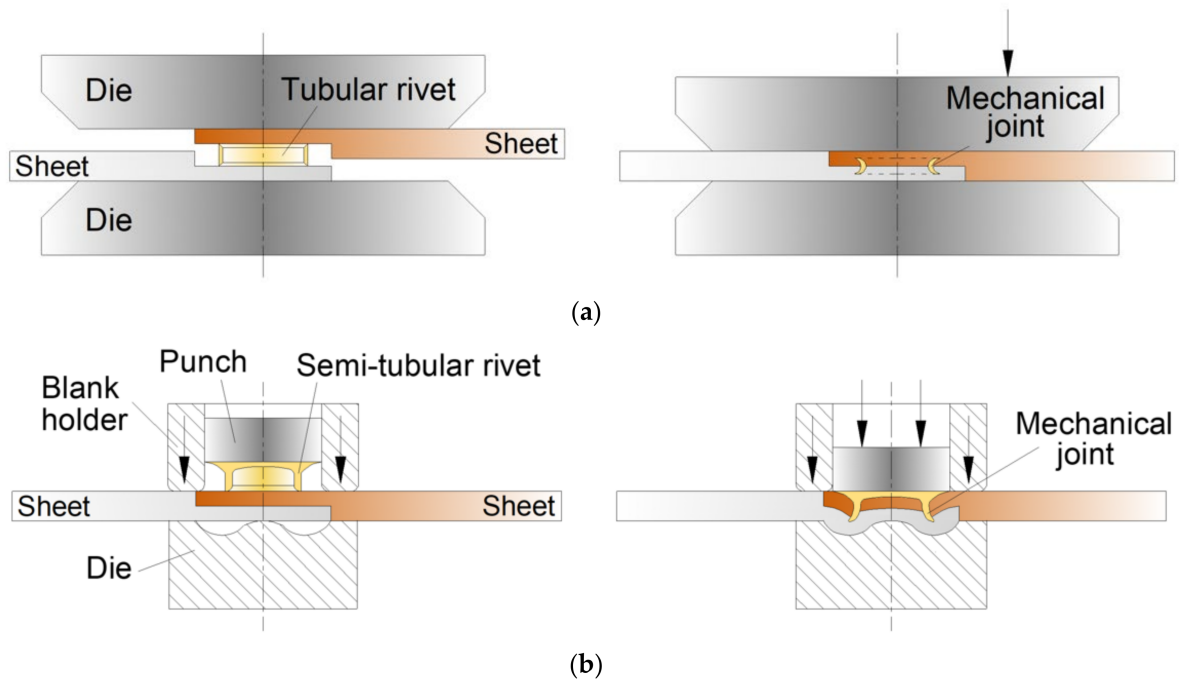


Figure 1. Schematics of (a) double-sided and (b) conventional self-pierce riveting.

Thus, DSSPR allows the joining of different and larger thicknesses with an easier tool system that is entirely made of just two flat compression plates (see Figure 1a), while keeping lower levels of force and energy. The simplicity of DSSPR has important benefits over SPR, since the rivet and die shapes of the SPR process have a big influence on the joint properties [10–15]. The sheet thickness also plays an important role in the fatigue [16] and corrosion performance [17,18] of SPR joints. Thicker sheets joined by SPR tend to fail either at the bottom sheet along the joint button or due to rivet damage or failure, while thinner sheets present poor durability in corrosive environments. Additionally, for the connection of dissimilar materials by SPR, access needs to be guaranteed to the softer sheet where the penetration of the rivet must be initiated, as shown in reference [19] for an aluminium–copper connection. There is then a compromise that limits the utilization of the SPR technology, despite the different strategies developed to ensure its application for joining multi-material structures and advanced materials [9].

In this research, different experimental specimens were produced with DSSPR to produce butt joints from half-lap joints, in an effort to overcome the constraints of butt joints, while improving the performance of Al-Cu connections and maintaining a constant thickness, typically required in some electrical and mechanical applications.

The specimens were subjected to different tests to analyse the mechanical and electrical performance of the mechanical joint. The latter is evaluated by means of the evolution of the electrical resistance with different working temperatures ranging from 16 °C to 100 °C. Comparisons are then made with fastened Al-Cu busbar connections [20,21] to evaluate and discuss the gains resulting from the utilization of DSSPR to produce busbar connections.

2. Materials and Methods

Tubular rivets of stainless-steel AISI 304 were employed to produce the half-lap joints between aluminium AA5754 and copper C11000 sheets. The sheets had a width w of 50 mm and an initial thickness t_0 of 5 mm, and they were machined halfway until a thickness t_i of 2.5 mm and an overlapped length L of 25 mm was produced. The rivets were machined from stainless-steel tubes and their parameters were selected to match the thickness t_i to be joined according to previous works [7,8]. These parameters are the external diameter d_0 , height h_0 , thickness t_0 and chamfered angle α , whose corresponding values were 10 mm, 5 mm, 1.5 mm and 45° , respectively.

To obtain the mechanical behaviour of the different materials, whose curves are presented in Figure 2, tensile and stack compression tests were carried out at room temperature in an INSTRON SATEC 1200 kN universal testing machine according to the corresponding standards [22,23]. The specimens were retrieved from the raw material of the different geometries utilized in this research, being extracted from the sheets to obtain the material flow curve for smaller values of strain with tensile tests [22], whereas for larger values of strain, cylindrical specimens were extracted from the same sheets, piled up and then subjected to stack compression tests [23]. Due to the smaller size and shape of the rivet, only the stack compression tests were utilized to obtain the material flow curve.

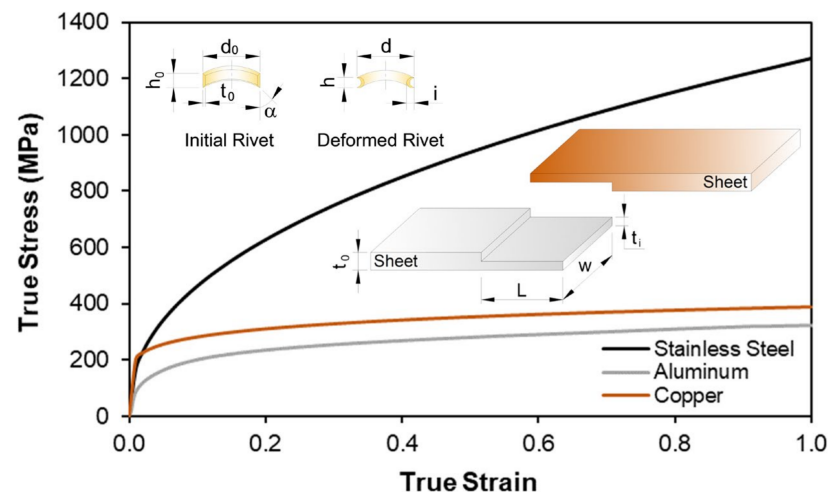


Figure 2. Material flow curves of the different geometries and respective process parameters.

The different unit cells were manufactured according to the specifications of the inserts in Figure 2. The joining process was performed in a single or a double stroke at room temperature, either by placing the rivet directly between the sheets and compressing them into each other or by pre-riveting the harder copper sheet and then riveting the aluminium sheet in a secondary stage. This produced significant differences, as predicted by the work previously carried out by the authors in [6,7], and it will be further discussed in a following section. Some joints were cut lengthwise to measure the parameters of the deformed rivet that are presented in Figure 2, such as the final height h and diameter d and the resulting mechanical interlocking i .

The setup utilized for the validation of the mechanical and electrical performance is presented in Figure 3. The DSSPR riveted joints were initially produced in the previously mentioned testing machine with a crosshead speed of 5 mm/min. They were then subjected to shear destructive tests (Figure 3a) according to the ISO 12996:2013 standard [24], in order to evaluate the maximum force that the joint can withstand before separation of the joint starts to occur. These tests were carried out in an INSTRON 4507 universal testing machine with a crosshead speed of 5 mm/min.

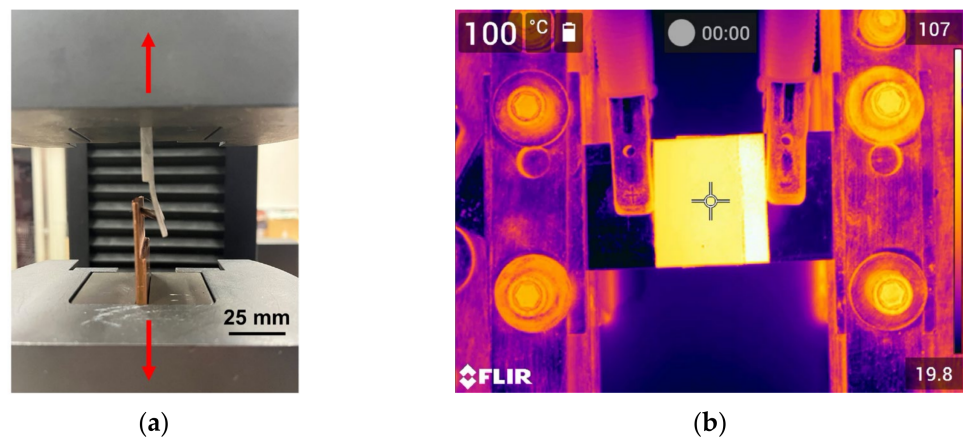


Figure 3. Setup utilized for (a) the tensile shear tests and for (b) the measurement of the electrical resistance with the corresponding temperature distribution provided by a thermal camera. In (b), the copper sheet is positioned on the left side and the aluminium sheet on the right side.

The riveted unit cells were also introduced in a setup composed of two copper plates in each side to clamp the riveted unit cell and were then connected to an OFICEL 1.5 kVA AC/DC transformer, responsible for heating the unit cell up to a maximum temperature of 105 °C (Figure 3b). During the cooling stage, the AC transformer was disconnected, and two probes were secured to the unit cell and connected to a KoCoS PROMET R600 micro-ohmmeter, as the unit cell cools off through heat exchange with the environment. This equipment allowed us to obtain the electric resistance at each temperature, which was monitored at each time using an FLIR E86 thermal imaging infrared camera. To ensure the same values of emissivity and guarantee the accuracy of the temperature measurements, the assessment region was painted in black (refer to Figure 3b). The probes were spaced 100 mm apart at the ends of the assessment region and a direct electric current of 600 A was passed for a few seconds each time a measurement took place. The measurements were made after a temperature drop of 20 °C between two successive measurements was observed until a temperature of 20 °C was finally reached.

3. Results

Joining Process

The unit cells were initially riveted in a single step that started with a single rivet being placed between the sheets, which were then pressed together. Due to the larger resistance of the copper material, the amount of rivet penetration in that sheet was very reduced in comparison with the aluminium sheet (Figure 4a). In fact, during the joining process, the rivet is unable to penetrate the copper sheet at the same rate of the aluminium sheet, and, in turn, the amount of penetration at the aluminium side becomes higher until a point where the strain hardening levels produced in the aluminium sheet force the rivet to flare [6,7]. This resulted in a weaker joint, not only in terms of its mechanical resistance but also in terms of the electrical resistance, since under these conditions, proper contact between the sheets and rivet was not guaranteed.

In a second iteration, a dedicated compression tool consisting of a bolster and a conical punch was employed to force the tubular rivet through the copper sheet (refer to the detail of Figure 4b). This ensures that the rivet is able to produce an adequate penetration in the copper sheet, and this strain-hardened region will motivate the subsequent deformation to occur mostly in the free region of the opposite rivet end, which is to be connected to the aluminium sheet.

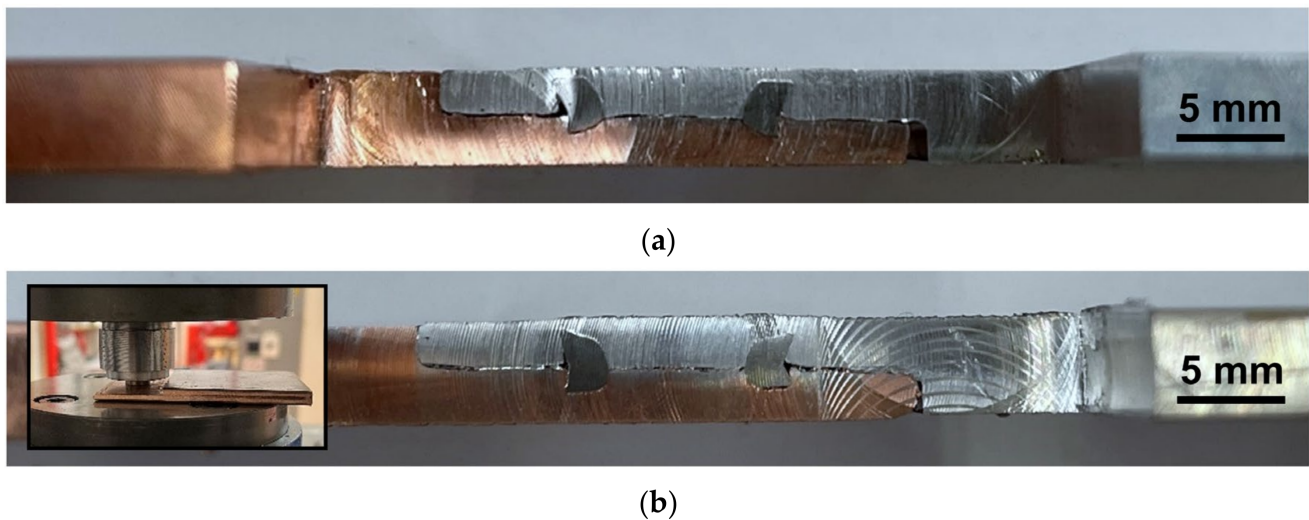


Figure 4. Details of the cross-section of the riveted joints obtained (a) without and (b) with a pre-riveting operation (with a detail of the pre-riveting tool).

The cross-section of the resulting riveted joint can be seen in Figure 4b, and in comparison with the result in Figure 4a, it can be observed that the amount of rivet penetration in the copper sheet was now increased with the same rivet parameters. In fact, the rivet penetration at the copper sheet increased by approximately 0.2 mm to a total of around 1.06 mm, whereas the rivet penetration in the aluminium sheet was reduced by approximately 0.06 mm to a total of around 1.47 mm. Most importantly, the rivet penetration was complemented by a significant increase in the rivet interlocking i in the copper sheet, which increased by approximately 0.32 mm, when previously it was almost inexistent. An increase in the rivet interlocking i in the aluminium sheet of around 0.02 mm was also observed in the pre-riveted joint. The increase in both the rivet penetration and interlocking prove the success of this strategy.

The DSSPR joint obtained with a pre-riveting operation of the copper sheet is presented in the graph in Figure 5, where the two different perspectives allow us to conclude that a butt joint can be successfully produced from a half-lap joint. This resulted in an enlarged contact surface that is not only limited to the side wall of the sheets, and consequently, will increase the strength of the joint that will now be able to withstand higher forces and bending moments. At the same time, the wider contact surface contributes to optimize both the thermal exchanges and the electrical resistance.

A successful connection is therefore obtained while preserving the original thickness of the raw sheets. The joining process is only revealed by the very small protrusion created at both sheet surfaces, which resulted from the material flow of the rivet inside the sheets during the riveting operation.

In terms of the overall joining force to produce the DSSPR joints, a maximum force of around 85 kN was registered for the pre-riveting operation, whereas for the second joining operation, a maximum force of around 135 kN was verified. The differences in the trends of the graph in Figure 5 for both joining stages are more noticeable for larger displacement values, where the strain hardening effect becomes more pronounced. In turn, an increase in the overall force and energy levels is observed as the flaring of the rivet ends takes place, until the sheets are in contact with each other and the joining process is completed.

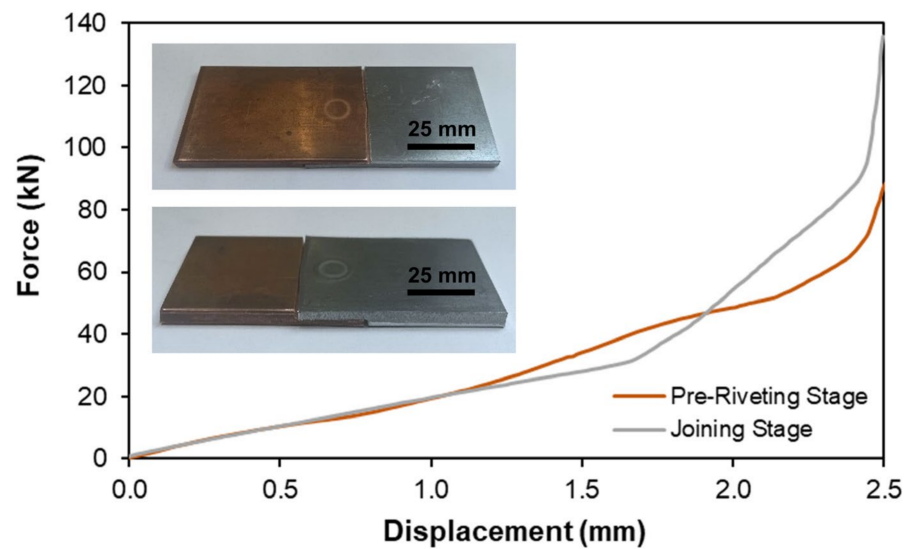


Figure 5. Evolution of force with displacement for the pre-riveting and joining stages. The respective mechanical joint is presented in the photographs included from two different perspectives.

4. Discussion

4.1. Mechanical Performance

During the tensile shear destructive tests, the detachment of the rivet from the sheets starts to occur in the sheet of lower mechanical strength, which is the aluminium sheet for this case. Instead of shearing, the prevailing failure mechanism in these tests was based on the bending and detachment of the tubular rivet from the sheets. The average results of these destructive tests are shown in the graph of Figure 6, where it can be observed that after a maximum force of approximately 5.2 kN, the separation of the joint started to occur.

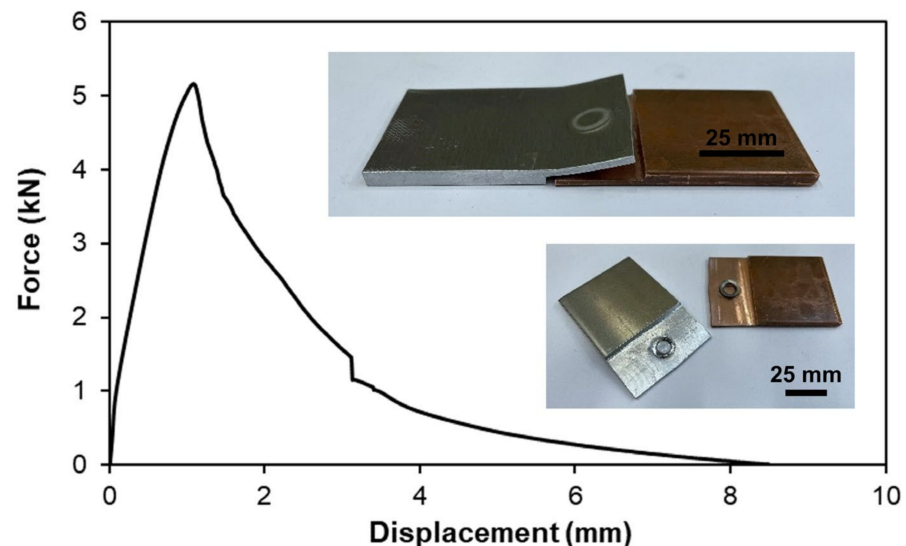


Figure 6. Force–displacement evolution for the shear destructive tests of the riveted joints from which resulted the specimens whose photographs are also included.

For reference purposes, an Al–Al riveted joint made from sheets with a thickness of 1.5 mm withstands a maximum force of around 2.2 kN [8], while for sheets with a thickness of 5 mm, the maximum force is around 10.2 kN [6]. Since a thickness of 2.5 mm is here subjected to tensile loads and the detachment occurs in the aluminium sheet, the maximum force value registered is in accordance with the expected performance of the DSSPR process.

As the unit cell is forced to separate, the sheet of lower mechanical strength is heavily deformed in the riveted region, as a consequence of the bending moment generated (refer to Figure 3a), to allow the detachment of the sheet from the rivet, as seen in the photographs in Figure 6. In contrast, the copper sheet remains undeformed, as does the rivet, which stays attached to that sheet after the mechanical joint is destroyed.

4.2. Electrical Performance

To assess the electrical performance of the riveted joint, the electrical resistance of the unit cells was measured for different temperatures, whose distributions are presented in Figure 7. These temperature distributions were obtained with the thermal imaging infrared camera.

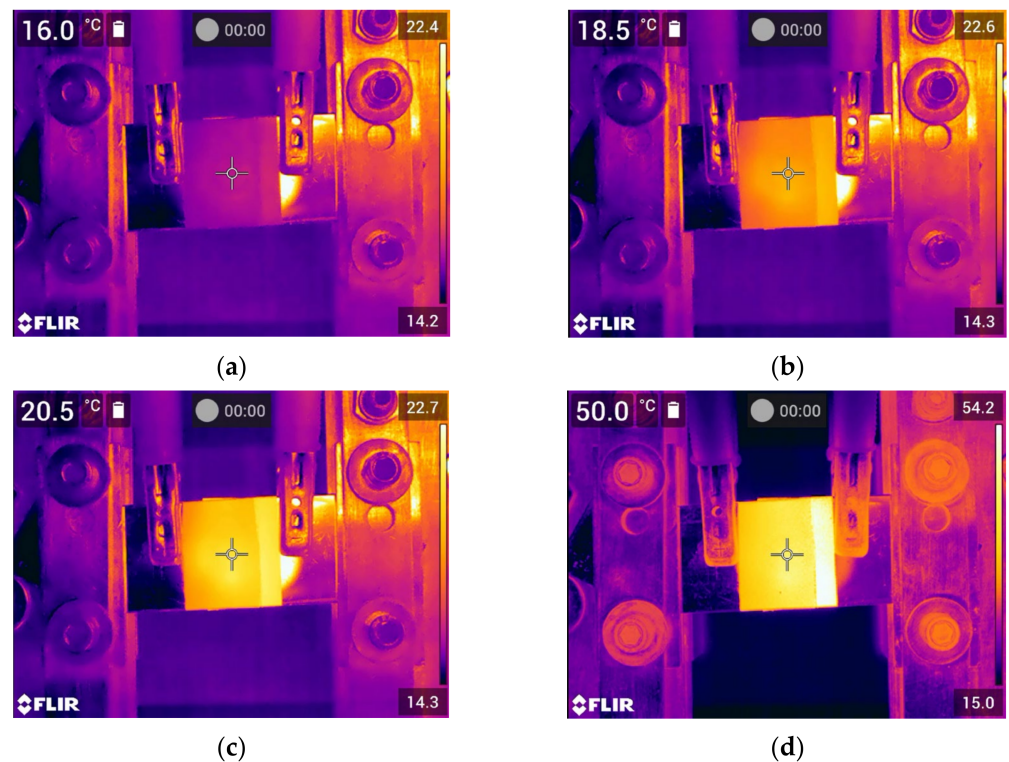


Figure 7. Temperature distribution for temperatures at the centre mark of (a) 16.0 °C, (b) 18.5 °C, (c) 20.5 °C and (d) 50.0 °C. The copper sheet is positioned on the left side whereas the aluminium sheet is positioned on the right side.

Looking at the evolution from Figure 7a (at room temperature) to Figure 7b (at 18.5 °C), it can be observed that the passage of electric current is developed in the annular region of the deformed rivet where the applied normal pressure is at its maximum due to the mechanical interlocking created by DSSPR. After an increase of 2 °C (Figure 7c), the passage of electric current in that location becomes more noticeable, and afterwards, the temperature distribution becomes homogeneous (Figure 7d).

Although the electric resistivity of the stainless-steel rivet is considerably higher than that of the aluminium sheet and even higher than of the copper sheet, the level of pressure generated by the joint allows us to maintain a nearly constant value of electrical resistance, as shown in Table 1. In comparison with fastened overlapped joints composed of a bolt and nut that brace the sheets from their two external surfaces, the normal pressure levels were evidently larger, and as a result, the electrical resistance was now slightly smaller for some of the tested temperatures after an electric current of 1500 A was also applied. Nevertheless, an overall range of around 5 $\mu\Omega$ was observed for the electrical resistance measured at the fastened joints, in comparison with a range of around 1.1 $\mu\Omega$ measured at the riveted joints (refer to Table 1).

Table 1. Summary of the measured electrical resistance at different temperatures for riveted and fastened joints [10].

Temperature (°C)	Riveted Joint	Fastened Joint
	Electrical Resistance ($\mu\Omega$)	Electrical Resistance ($\mu\Omega$)
100	23.71	24.00
80	23.59	23.00
60	23.09	21.00
40	23.28	20.00
20	24.19	19.00

The increase in the electrical resistance with the increase in temperature for fastened joints can be related to the stretching of the bolt and nut, which is directly linked to the higher resistivity of the steel in comparison with the remaining materials. This results in a reduction in the contact area between the sheets, which is associated with the significant increase in the electrical resistivity of steel for larger temperatures and leads to an increase in the electrical resistance according to Equation (1), where the electrical resistance R is written as function of the electrical resistivity ρ and of the ratio between the contact length L and contact area A .

$$R = \rho \frac{L}{A} \quad (1)$$

For larger levels of electric current and voltage to which the fastened joints may be subjected in working conditions, the risk of fracture is increased due to the occurrence of thermal fatigue resulting from expansion and contraction of the bolt, which is related to the significant differences in its electric resistivity for different temperatures [10]. In the riveted DSSPR joints, this phenomenon also occurs but is now limited by the aluminium and copper sheets, whose smaller electrical resistivity counteracts these movements. Also, the smaller size of the rivet avoids larger expansion–contraction cycles and therefore the riveted joint stays more tight. As a result, the electrical resistance of the riveted joint remains almost unchanged for different temperatures and eliminates the probability of critical defects occurring during the service life of the joints.

It is also worth mentioning that the contact surface of the riveted unit cells is that resulting from the machining operation utilized to reduce the sheet thickness at the joining location, and therefore smaller values of electrical resistance can still be achieved for these riveted joints in comparison with the fastened overlapped joints, which utilized the virgin surfaces of the supplied sheets.

The effectiveness of the riveted joint is also proved by the fact that although the overlapped contact length L is half of that utilized in the fastened joint [21], the differences in the measured electrical resistance are not significant, which indicates an increased contact area produced by the riveted joint, which is responsible for compensating for the significant reduction in the contact length. Also, it was seen in [21] that the tightening torque of the bolt and nut in the fastened joint has a substantial impact on the contact pressure and consequently on the electrical resistance, which can be severely compromised by the self-loosening of the fastened joint during its service life.

5. Conclusions

The utilization of DSSPR proved to be successful in producing Al-Cu connections of constant thickness, which are very useful for busbar connections. This was possible through the utilization of half-lap joints to replicate butt joints, commonly utilized in these electrical applications, in an effort to increase the contact area, which is essential to reduce the electrical resistance and thus the heat generated in those Al-Cu joints.

A pre-riveting operation of the copper sheet and the subsequent joining to the aluminium sheet guaranteed a sound joint with adequate penetration of each sheet, despite the significant differences in the mechanical strengths of these materials. The mechanical performance of the joint produced is in line with the previous tests performed with the

riveting technology, and as expected, the failure of the joint is triggered by the deformation of the softer sheet to allow the detachment of the rivet.

In comparison with conventional fastened joints, the riveted DSSPR joints produce a constant electrical resistance across different temperatures, since the effects of the higher resistivity of the steel material and the geometrical changes that it produces in the rivet are constrained by the aluminium and copper sheets. It was also seen that the normal pressure created by the rivet is much larger than a fastened joint and not dependent on the tightening torque of the bolt and nut.

Further developments to lower the electrical resistance of the joint may still be achieved with a proper control of the surface finish, such as the reduction in the surface roughness and the elimination of contaminants and oxide films.

Author Contributions: Conceptualization, R.M.A.; Data curation, R.M.A.; Formal analysis, R.M.A. and L.M.A.; Investigation, R.M.A. and L.M.A.; Methodology, R.M.A.; Supervision, R.M.A.; Validation, R.M.A. and L.M.A.; Visualization, R.M.A.; Writing—original draft, R.M.A.; Writing—review and editing, R.M.A. and L.M.A. All authors have read and agreed to the published version of the manuscript.

Funding: This research was supported by the Fundação para a Ciência e a Tecnologia of Portugal and IDMEC under LAETA-UIDB/50022/2020 and PTDC/EME-EME/0949/2020.

Data Availability Statement: Not applicable.

Acknowledgments: The authors would like to acknowledge the support provided by IDMEC and the Fundação para a Ciência e a Tecnologia of Portugal.

Conflicts of Interest: The authors declare no conflict of interest. The funders had no role in the design of the study; in the collection, analyses, or interpretation of data; in the writing of the manuscript or in the decision to publish the results.

References

1. Materion. Available online: <https://materion.com/markets/automotive/hybrid-batteries> (accessed on 21 June 2023).
2. Verweij, A.P. Busbar and Joints Stability and Protection. In Proceedings of the Chamonix Workshop on LHC Performance, Chamonix, France, 2–6 February 2009; pp. 113–119.
3. DIN 8593-5:2003-09; Manufacturing Processes Joining—Part 5: Joining by Forming Processes; Classification, Subdivision, Terms and Definitions. DIN—German Institute for Standardization: Berlin, Germany, 2003.
4. Meschut, G.; Merklein, M.; Brosius, A.; Drummer, D.; Fratini, L.; Füssel, U.; Gude, M.; Homberg, W.; Martins, P.A.F.; Bobbert, M.; et al. Review on mechanical joining by plastic deformation. *J. Adv. Join. Process.* **2022**, *5*, 100113.5. [[CrossRef](#)]
5. Buffa, G.; Fratini, L.; La Commare, U.; Römisch, D.; Wiesenmayer, S.; Wituschek, S.; Merklein, M. Joining by forming technologies: Current solutions and future trends. *Int. J. Mater. Form.* **2022**, *15*, 27. [[CrossRef](#)]
6. Afonso, R.M.; Alves, L.M. Joining Strategies for Double-Sided Self-Pierce Riveting. *Materials* **2023**, *16*, 1191. [[CrossRef](#)] [[PubMed](#)]
7. Alves, L.M.; Afonso, R.M.; Pereira, P.T.; Martins, P.A.F. Double-sided self-pierce riveting of dissimilar materials. *J. Adv. Manuf. Technol.* **2021**, *115*, 3679–3687. [[CrossRef](#)]
8. Alves, L.M.; Moghadam, M.; Afonso, R.M.; Nielsen, C.V.; Martins, P.A.F. On the applicability limits of double-sided self-pierce riveting. *Proc. Inst. Mech. Eng.* **2022**, *236*, 2027–2036. [[CrossRef](#)]
9. Kappe, F.; Wituschek, S.; Bobbert, M.; Lechner, M.; Meschut, G. Joining of multi-material structures using a versatile self-piercing riveting process. *Prod. Eng.* **2023**, *17*, 65–79. [[CrossRef](#)]
10. Huang, Z.C.; Zhou, Z.J.; Huang, W. Mechanical Behaviors of Self-Piercing Riveting Joining Dissimilar Sheets. *Adv. Mater. Res.* **2010**, *97–101*, 3932–3935. [[CrossRef](#)]
11. Haque, R.; Durandet, Y. Investigation of self-pierce riveting (SPR) process data and specific joining events. *J. Manuf. Process.* **2017**, *30*, 148–160. [[CrossRef](#)]
12. Haque, R. Quality of self-piercing riveting (SPR) joints from cross-sectional perspective: A review. *Arch. Civ. Mech. Eng.* **2018**, *18*, 83–93. [[CrossRef](#)]
13. Ang, H.Q. An Overview of Self-piercing Riveting Process with Focus on Joint Failures, Corrosion Issues and Optimisation Techniques. *Chin. J. Mech. Eng.* **2021**, *34*, 2. [[CrossRef](#)]
14. Abe, Y.; Kato, T.; Mori, K. Joinability of aluminium alloy and mild steel sheets by self piercing rivet. *J. Mater. Process. Technol.* **2006**, *177*, 417–421. [[CrossRef](#)]
15. Karathanasopoulos, N.; Mohr, D. Strength and Failure of Self-Piercing Riveted Aluminum and Steel Sheet Joints: Multi-axial Experiments and Modeling. *J. Adv. Join. Process.* **2022**, *5*, 100107. [[CrossRef](#)]

16. Zhao, L.; He, X.; Xing, B.; Lu, Y.; Gu, F.; Ball, A. Influence of sheet thickness on fatigue behavior and fretting of self-piercing riveted joints in aluminum alloy 5052. *Mater. Des.* **2015**, *87*, 1010–1017. [[CrossRef](#)]
17. Calabrese, L.; Proverbio, E.; Bella, G.D.; Galtieri, G.; Borsellino, C. Failure behaviour of SPR joints after salt spray test. *Eng. Struct.* **2015**, *82*, 33–43. [[CrossRef](#)]
18. Hönsch, F.; Domitner, J.; Sommitsch, C.; Götzinger, B. Modeling the Failure Behavior of Self-Piercing Riveting Joints of 6xxx Aluminum Alloy. *J. Mater. Eng. Perform.* **2020**, *29*, 4888–4897. [[CrossRef](#)]
19. He, X.; Zhao, L.; Deng, C.; Xing, B.; Gu, F.; Ball, A. Self-piercing riveting of similar and dissimilar metal sheets of aluminum alloy and copper alloy. *Mater. Des.* **2015**, *65*, 923–933. [[CrossRef](#)]
20. Hadzhiev, I.; Malamov, D.; Balabozov, I.; Yatchev, I. Analysis of the influence of some factors on the contact resistance of bolted busbar connections. *IOP Conf. Ser. Mater. Sci. Eng.* **2019**, *618*, 012025. [[CrossRef](#)]
21. Sampaio, R.F.V.; Pragana, J.P.M.; Bragança, I.M.F.; Silva, C.M.A.; Martins, P.A.F. Thermo-electrical performance of hybrid busbars: An experimental and numerical investigation. *Proc. Inst. Mech. Eng. Part L J. Mater. Des. Appl.* **2022**, *237*, 70–80. [[CrossRef](#)]
22. *ASTM E8/E8 M*; Standard Test Methods for Tension Testing of Metallic Materials. ASTM International: West Conshohocken, PA, USA, 2016.
23. Alves, L.M.; Nielsen, C.V.; Martins, P.A.F. Revisiting the fundamentals and capabilities of the stack compression test. *Exp. Mech.* **2011**, *51*, 1565–1572. [[CrossRef](#)]
24. *ISO 12996:2013*; Mechanical Joining—Destructive Testing of Joints—Specimen Dimensions and Test Procedure for Tensile Shear Testing of Single Joints. ISO—International Organization for Standardization: Geneva, Switzerland, 2013.

Disclaimer/Publisher’s Note: The statements, opinions and data contained in all publications are solely those of the individual author(s) and contributor(s) and not of MDPI and/or the editor(s). MDPI and/or the editor(s) disclaim responsibility for any injury to people or property resulting from any ideas, methods, instructions or products referred to in the content.